

See discussions, stats, and author profiles for this publication at: <https://www.researchgate.net/publication/339775027>

# Simulink model of transformer differential protection using phase angle difference based algorithm

Article in *International Journal of Power Electronics and Drive Systems* · June 2020

DOI: 10.11591/ijpeds.v11.i2.pp1088-1098

CITATIONS

3

READS

928

2 authors:



**Nassim Iqteit**

Palestine Polytechnic University

13 PUBLICATIONS 21 CITATIONS

[SEE PROFILE](#)



**Khalid Yahya**

Gelisim Üniversitesi

26 PUBLICATIONS 84 CITATIONS

[SEE PROFILE](#)

Some of the authors of this publication are also working on these related projects:



DEVELOPMENT AN EFFICIENT MAXIMUM POWER POINT TRACKER FOR THERMOELECTRIC GENERATORS UNDER VARIOUS CONDITIONS [View project](#)



Minimizing power losses in distribution system [View project](#)

## Simulink model of transformer differential protection using phase angle difference based algorithm

Nassim A. Iqteit<sup>1</sup>, Khalid Yahya<sup>2</sup>

<sup>1</sup>Department of Electrical Engineering, Palestine Polytechnic University, Palestine

<sup>2</sup>Department of Mechatronic Engineering, Istanbul Gelisim University, Turkey

---

### Article Info

#### Article history:

Received Sep 3, 2019

Revised Nov 9, 2019

Accepted Feb 16, 2020

---

#### Keywords:

Differential relay

Inrush current

Internal fault

Phase angle difference

---

### ABSTRACT

An application of phase-angle-difference based algorithm with percentage differential relays is presented in this paper. In the situation where the transformer differential relay is under magnetizing inrush current, the algorithm will be utilized to block the process. In this study, the technique is modeled and implemented using Simulink integrated with MATLAB. The real circuit model of power transformer and current transformers are considered in the simulation model. The results confirmed the effectiveness of the technique in different operation modes; such as, magnetizing inrush currents, current transformers saturation and internal transformer faults.

*This is an open access article under the [CC BY-SA](https://creativecommons.org/licenses/by-sa/4.0/) license.*



---

### Corresponding Author:

Nassim A. Iqteit,

Department of Electrical Engineering,

Palestine Polytechnic University,

Hebron-Wadi Alharea Building PO BOX: 198, Palestine.

Email: [nassim\\_eng83@ppu.edu](mailto:nassim_eng83@ppu.edu)

---

## 1. INTRODUCTION

Transformers are a vital and expensive component of electrical power systems. The protection of transformers is essential to achieve high quality performance in modern electric networks. The winding faults on power transformers caused by high sensitivity, selectivity and fast response will be deterred by the differential protection relay [1]. Transformers with a high capacity are usually protected by a harmonic restraint percentage differential relay [2]. The faults that occur in transformers are either: internal incipient faults or internal short circuit faults [3]. Short circuit faults constitute about 70-80% of transformer failures, and these can be (1) phase-to-ground fault or (2) turn-to-turn faults [4].

Due to the nonlinearities in the transformer core, or in the CT core or in both case a substantial differential current may flow, when there is no fault. These false differential currents are generally sufficient to cause a percentage differential relay to trip. Some of these phenomena are magnetizing inrush current during energization or fault removal, transformer over-excitation and CT saturation. However, in modern digital relays some algorithms were developed to avoid the false tripping in percentage differential relays. Some of these algorithms have been developed based on different techniques, such as, artificial neural networks, fuzzy logic, wavelet transforms and principal component analysis [5-8]. These approaches have limitations that may affect their speed of operation, dependability and security. They also require complex computations and are susceptible to changes in transformer parameters.

The differential protection on magnetizing inrush currents can be averted by many effective methods [9-12]. One of those methods is making the phase voltage as a control signal. And this way guarantee that the protected transformer is explicitly decreased in the terminal voltage. Also, implementing a core-flux or transformer which is equivalent circuit for electing inrush from internal fault currents could be another remarkable method. Those ways could achieve major success concerning their applications if the transformer terminal voltage measured and the measurement process will be quite costly [13]. Additionally, computational burden on the differential relay would be increased so that causes a slow motion in winding short circuits [14-16].

Phase angle difference technique, proposed by [1] is used to avoid limitations in previous techniques, and to improve the reliability and fast response in percentage differential relay. In this paper to discriminate magnetizing inrush currents and short circuit faults in power transformer, the PAD technique with percentage differential relays will be modeled and simulated using Simulink package in MATLAB software. Also, the real circuit model of power transformer and CTs transformer will be considered in the simulation model in both cases.

## 2. METHODOLOGY OF DIFFERENTIAL RELAY WITH PAD

### 2.1. Percentage differential (87T) characteristic

Power transformers that are rated above 10 MVA are most commonly protected with percentage differential relay (87T) for the purposes of avoiding internal short circuits. The 87T-relay has been found to offer important ground and speed phase protection for 2 and 3 winding power transformers [17]. The relay features an additional harmonics restraint unit in which massive transformer magnetizing inrush is present as well as ratio matching taps. The unit prevents relay operation on transformer magnetizing inrush current. The second harmonics restraint unit is factory calibrated to restrain 15% second harmonic current, but may be adjusted if required. An unrestrained instantaneous unit which operates on magnitude of difference current is provided to back up the percentage differential unit. The unit is adjustable from approximately 8 to 20 times tap [18]. The characteristic of percentage differential relay is providing following in Figure 1 [19, 20]. The characteristic In this case the differential current is false, they still can cause a trip in a percentage differential relay. Sometimes during energization inrush current is magnetized. The situation can also occur during transformer over-excitation, or fault removal, or CT saturation. However, recently, algorithms have been developed to avoid the false tripping in percentage differential relays. Various techniques such as principal component analysis, fuzzy logic and artificial neural networks helped to to develop these algorithms. These techniques have their parameters in Figure 1 are as follows:

$I_{diff}$ : is magnitude of 50 Hz component for differential current.

$I_{res}$ : is magnitude of 50 Hz component for restraint current.

$I_{op1}$ : is the minimum operation current.

$I_{op2}$ : is the adjusted minimum operating current

$I_{res, min}$ : is minimum restraint current.

$k$ : gradient of the functional characteristic which are, 10, 20 or 40%.

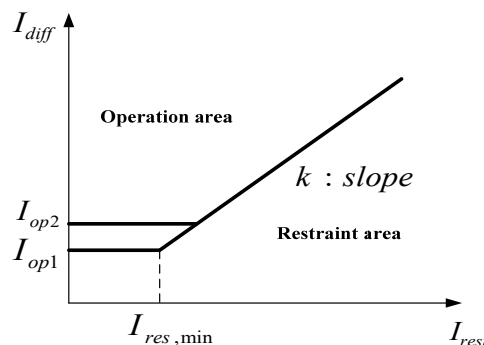


Figure 1. Percentage differential relay (87T) characteristic

$I_{diff}$  with transformation ratio of  $n$  is defined by (1), while  $I_{res}$  at the same ratio is given by (2).

$$I_{diff,\phi} = |\vec{I}_{1,\phi} - \vec{nI}_{2,\phi}| \quad (1)$$

$$I_{res,\phi} = |\vec{I}_{1,\phi} + \vec{nI}_{2,\phi}|/2 \quad (2)$$

Where,

$\vec{I}_{1,\phi}$ : is transformer primary current at phase  $\phi$  (namely, A, B or C).

$\vec{nI}_{2,\phi}$ : is transformer secondary current at phase  $\phi$  (namely, A, B or C).

The percentage differential operating characteristic prevents operation until the differential current is greater than a certain percentage of through current. (3) as shown provides the operating characteristic of one phase differential element. The threshold value  $I_{op1}$  biases the differential operating current. The threshold value must be chosen based on the magnetizing current's magnitude, and the differential current, which results from on-load tap-changing which occurs during normal transformer loading conditions [21, 22]. The second inequality models the slope of the transformer differential relay.

$$\left\{ \begin{array}{l} I_{diff} \geq I_{op1} \\ I_{diff} \geq k(I_{res} - I_{res,min}) + I_{op1} \end{array} \right\} \quad (3)$$

The minimum operating current  $I_{op1}$  in amperes can be calculated with the following relation [11]:

$$I_{op1} = \frac{k}{1+k} \times R \times T \quad (4)$$

R: is adjustable min. restraint setting,  $R \in [1-3]$ .

T: is tap setting in amperes.

## 2.2. Fault discrimination techniques in power transformers

### 2.2.1. Transformer current transient components technique

The described technique is utilized to discern between external and internal faults within power transformers. The phase transient currents (all three) of the transformer go through conversion into the modal current components by way of Clarke's transformation to give ground mode I0, areal mode I1 as well as areal mode I2. High and low tension sides of the transformer give transient modal currents which are used with the Fault Discrimination Equation (FDE), which in turn is able to discern internal from external faults based on polarity of its output. The polarity of the FDE, for internal faults, will register negative whereas it will be largely positive for external faults. The following equation provides the fault discrimination equation:

$$FDE = average\{(I_0)_{th} \cdot (I_0)_{tl} + (I_1)_{th} \cdot (I_1)_{tl} + (I_2)_{th} \cdot (I_2)_{tl}\} \quad (5)$$

Where,

$(I_0)_{th}$ ,  $(I_0)_{tl}$ : are the currents (transient ground mode) on high and on low tension sides.

$(I_1)_{th}$ ,  $(I_1)_{tl}$ : are the currents (transient aerial mode) 1 on high and on low tension sides.

$(I_2)_{th}$ ,  $(I_2)_{tl}$ : are the currents (transient aerial mode) 2 on high and on low tension sides.

### 2.2.2. Fault detection process in power transformers applying the Discrete Wavelet Transform

The Discrete Wavelet Transform technique is used for on-line fault detection within power transformers. Wavelet technique is a time-scale domain approach, which is applied to locate short circuit faults and incipient faults through comparison of performance during normal operation of the power transformer. The following steps outline the fault detection algorithm [23]:

Step 1: Obtain and record current signals from power transformer terminals.

Step 2: Analyze the signal applying a wavelet taken from a wavelet family, for the required level of decomposition.

Step 3: Assess the approximate coefficients and detail of Discrete Wavelet Transform with time through firstly plotting a sample—coefficient graph.

Step 4: Locate the fault via wavelet coefficient interpretation.

Step 5: Differentiate fault current (incipient), from internal short circuit current and ordinary operation current.

Discrete wavelet transform is also a technique that is used. It can be applied together with back propagation neural networks and is applied to classify different internal fault types in a three-phase transformer [24].

**2.3. Phase angle difference (PAD) principle technique**

To differentiate the internal fault current from a different disturbance in a power transformer, the PAD in the fundamental frequency components will be used as the guide [25, 26]. It is not necessary that the exact PAD is used. The location of  $\theta$  relative to the PAD scheme operating characteristic can be estimated to find the status of a given power transformer. Figures 2 and 3 highlights that the operating mode of the power transformer is the main determinant of the principle of Phase Angle Difference. Under normal operation as well as in external fault, the line currents flow are parallel with the variance in phases being almost zero as shown Figures 2(b) and 2(e) respectively. However, during the magnetizing inrush currents, the PAD is approximately 90o since it is largely inductive as seen in Figure 2(a). Subjecting the transformer to winding short current reverses either, if the transformer is exposed to a winding short circuit, either I1 or nI2 current. In this case the PAD becomes greater than 90o in turn-to-turn fault and turn-to-ground fault as is visible in Figures 2(c) and 2(d). Now, through using Idiff and Ires, we can estimate PAD without placing much strain on the relay with great computations which would in turn slow its response. Figure 3 shows how to estimate PAD in a power transformer on different operation modes.

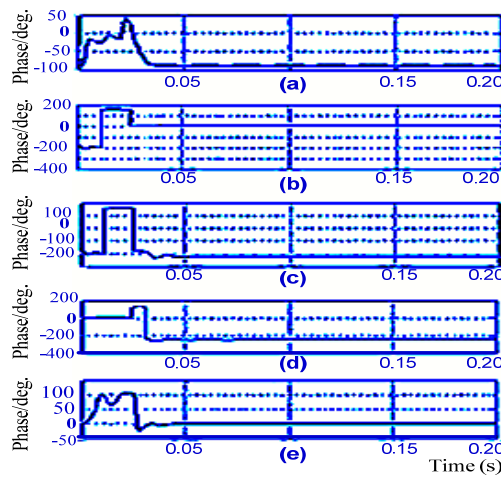


Figure 2. PAD between the 50Hz components of phase A respective currents. (a) Magnetizing inrush. (b) Normal loading. (c) Turn-to- ground fault (d) Turn-to-turn fault and (e) external fault (AC-G)

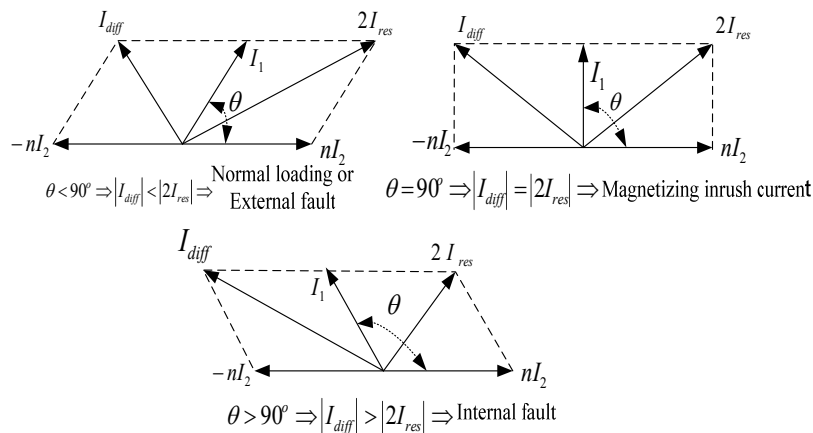


Figure 3. Phasor diagram for computing PAD respective line currents: Normal loading, external faults, magnetizing inrush and internal faults

### 3. MODELING OF POWER SYSTEM COMPONENTS

#### 3.1. Simulink model of power system

Figure 4 illustrates the power system's single-line diagram used in the study. The sources  $E_s \angle 0^\circ$  and  $E_r \angle \theta$  behind series impedances represent transmission and distribution networks. BA and BB are circuit breakers with resistance  $0.001 \Omega$ .

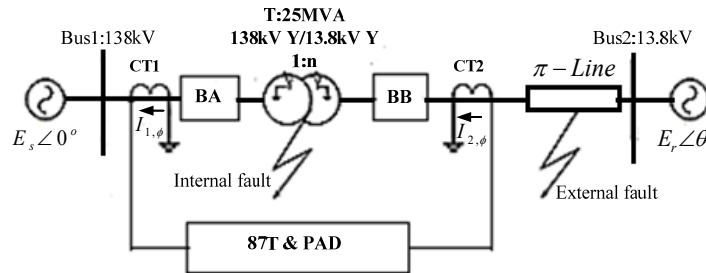


Figure 4. Single-line diagram of simulated power system

Figure 5 shows the Simulink model of the elements of the power system with the protection relay. The power system parameters in Figure 5 (a) are given in the Appendix. The power transformer in Simulink model in Figure 5(a), can be noted as in Y/Y together showing a grounded neutral together with a 25MVA rated capacity and 138kV/13.8kV rated voltages. As shown in Figure 5(b), the power transformer is modeled for calculating different operating modes, such as: internal faults, normal operation and magnetizing inrush currents. We can simulate the operations through power transformer control switches S1, S2, S3, S01 and S02 with BA and BB circuit breakers.

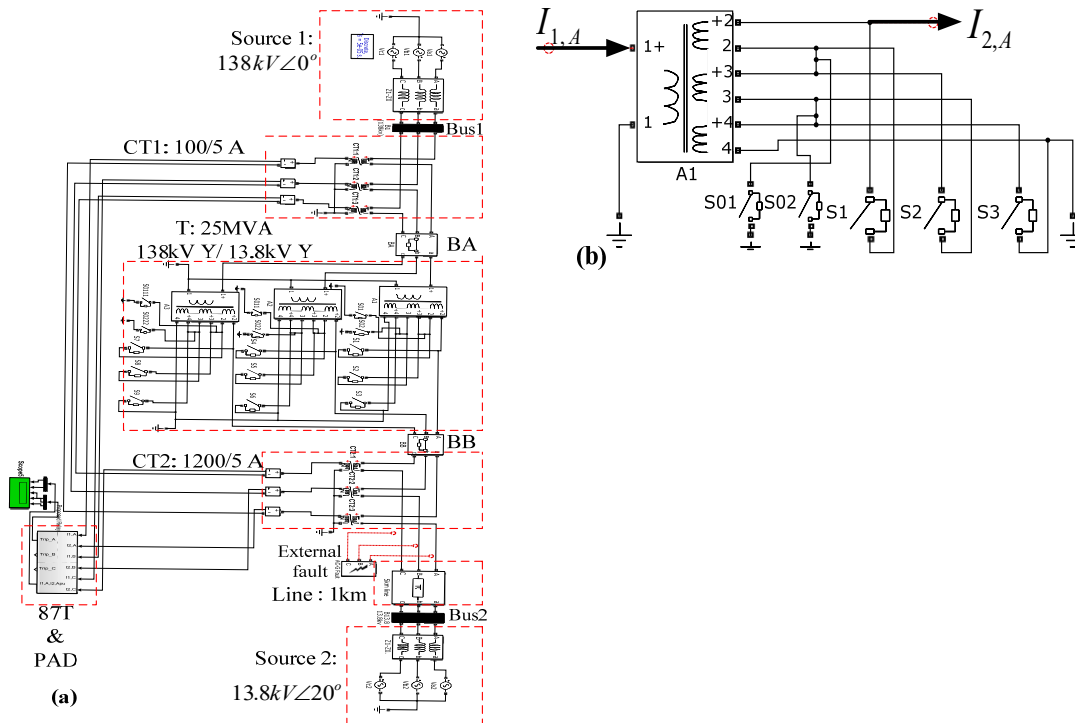


Figure 5. Power system with 87T relay and PAD scheme: (a) three phase diagram (Simulink model) and (b) Power transformer model (phase A)

The cores and windings of transformer is modeled by equivalent circuit illustrated in Figure 6(a). The (current– flux) characteristics of power transformer and CTs are shown in Figures 6(b) and 6(c). The calculations of transformer are referred to the relay side ( $I_1, nI_2$ ). A single  $\pi$ -section models the transmission line.

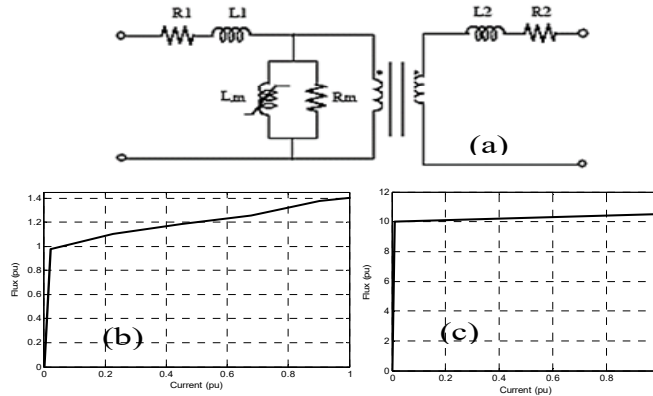


Figure 6. (a) Power transformer single phase equivalent circuit (b) Power transformer current– flux characteristics and (c) CTs current– flux characteristics

**3.2. Simulink model of PAD scheme and differential relay**

The developed differential relay with PAD scheme is implemented in Simulink software, for evaluating its performance at different operating conditions of the power transformer. A block diagrams of the proposed differential relay is shown in Figures 7 and 8. Figure 7 include amper 2pu block to convert the phase sampling currents from CT1&CT2 (phase A) to pu-values. The relay +PAD block of phase A represents the differential relay (87T) with associated PAD schemes. Scope1 in Figure 7 is only used to determine the phase angle difference between  $I_1, A$  and  $nI_2, A$ . The base current for the HV-side is 5.23 A, while the base current for the LV-side is 4.358 A.

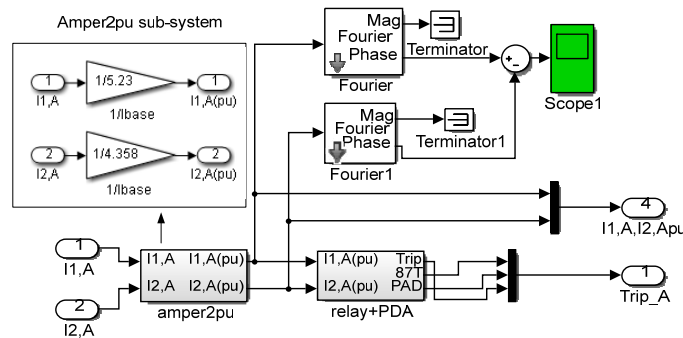


Figure 7. Simulink Block diagram of protection system (Phase A)

The model of percentage differential relay elements (phase-A elements) with PAD restraint scheme is depicted in Figure 8, where the magnitude values of  $I_{diff} (I_1-nI_2)$  and  $2I_{res} (I_1+nI_2)$  are computed using ‘Fourier analyzer’ Simulink model. The differential relay characteristics given by (3) are represented by comparators 2 and 3 along with Simulink embedded function  $f(u)$  to generate X and Y signals. The differential relay characteristic shown in Figure 1 has boundary values:  $I_{op1}$  is 0.2 pu ,  $I_{op2}$  is 0.3 pu,  $I_{res,min}$  is 0.6 pu and the slop k equal to 0.2. The differential element also involves instantaneous trip function using comparator 1 that creates the unrestraint signal UR if the condition:  $I_{diff} \geq 20$  pu, is satisfied. The PAD scheme is characterized by comparator 4 to produce blocking or releasing signal PAD according to

the tripping criterion of the scheme. The function  $f1(u)= Idiff -0.0001$  is used only as a correction function to correct some mismatch Simulink values. The output signal of AND1 gate is used to generate 87T differential relay signal. Finally, the output of OR gate is used to generate the final trip signal (Trip\_A)

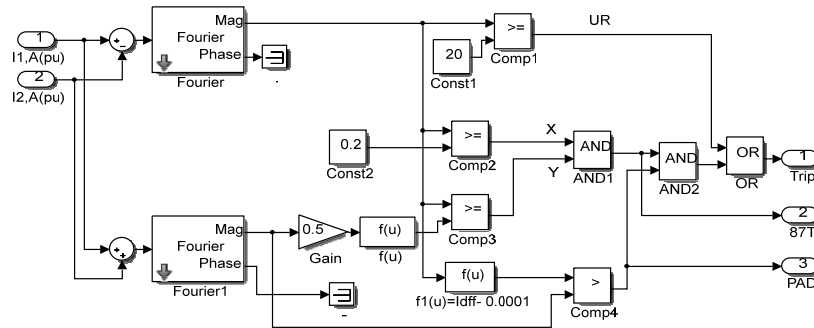


Figure 8. Differential relay (87T) with PAD scheme

#### 4. SIMULATION RESULTS AND ANALYSIS

The power transformer in Simulink model is simulated in normal loading, internal fault and external fault as well as magnetizing inrush operating modes. The following Figures 9-13 display the phase A secondary currents of CT1 (a), and CT2 (b) in pu values. The same figures show the output signal of 87T differential relay (c), PAD scheme (d), and final trip signal of phase A (e). The simulation time of our model is 200 ms.

##### 4.1. Power transformer with normal loading

In normal loading mode, the connected switches with power transformer are in ‘off’ position, and the breakers BA and BB are switched on 25 ms after the running program. In this mode of operation, the input currents to primary have the same direction of the current flow from the secondary of power transformer. For this reason, the output signals of 87T and PAD are zero causing the final trip to be zero, as shown in Figure 9.

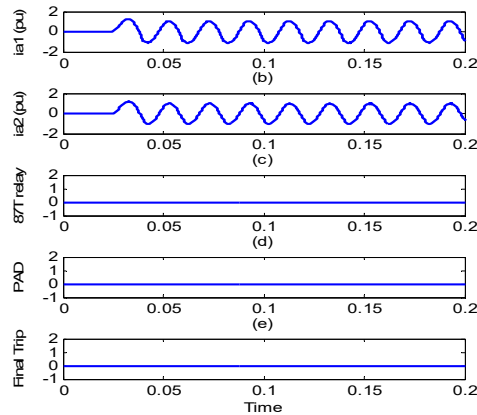


Figure 9. Response of the PAD-based algorithm to normal loading

##### 4.2. Power transformer with magnetizing inrush current

The transformer model is provided with a non-linear inductor  $L_m$  connected as shown in the Figure 6(a) for each phase.  $L_m$  is used to account magnetizing current representation. The power transformer characteristics (*current – flux*) of  $L_m$  are depicted in Figure 6(b). The magnetizing inrush current can be



simulated by switching off all switches and breakers on the LV side of power transformer, and closing circuit breaker BA. Figures 10(a) and 10(b) compares the proposed Simulink model and EMTP-RV simulation package [1] in the case of inrush currents, where the results were found close to each other. In the obtained results of Figure 10(a), the breaker BA was switched on after one cycle of running model. A magnetizing inrush current of amplitude up to 8 times the transformer rated current is simulated. It is obvious that such inrush current causes the mal-operation of the differential relay. Nevertheless, the output signal of PAD scheme is zero logic and the PAD decision is stable and independent of the magnitude of the inrush current. Finally, the transformer breakers will not trip.

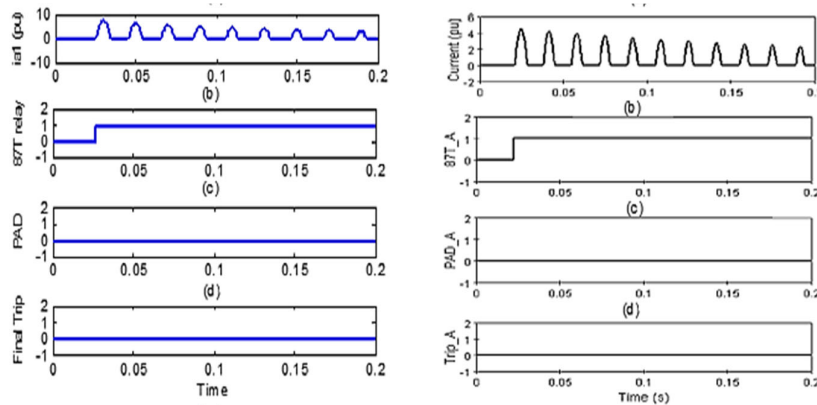


Figure 10. Response of the PAD-based algorithm to magnetizing inrush current, (a) Proposed Simulink model, (b) EMTP-RV simulation package [1]

**4.3. Power transformer with turn to ground fault**

Figure 11 presents the performance of the percentage differential relay 87T and the PAD scheme to a turn-to-ground fault occurred when the switches  $S_1$  &  $S_{01}$  are closed. Figure 11(a) shows the results of the proposed Simulink model whereas Figure 11(b) illustrates the results of using the EMTP-RV simulation package and applying PAD [1]. The results of both methods were similar to each other. The fault is initiated at time  $t = 25$  ms with zero fault resistance. Both differential relay and PAD scheme have the ability to detect the fault, but with different time instants as appeared in the figure. The different time instants is due to the utilization of Discrete Fourier Transform (DFT) for calculating the magnitude values of the differential and restraint currents. The final trip signal is released only for the faulted phase, leading to the disconnection of the power transformer from the total power system.

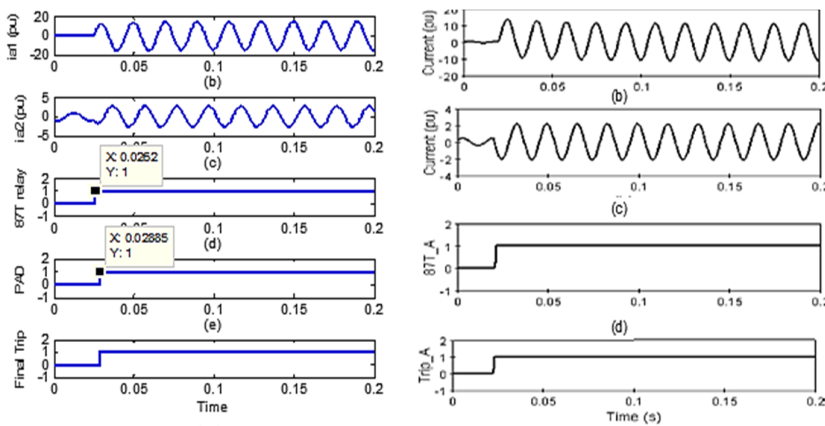


Figure 11. Response of the PAD-based algorithm to turn-to-ground fault. (A) Proposed Simulink model, (B) EMTP-RV simulation package [1]

#### 4.4. Power transformer with turn to turn fault

Turn-to-turn fault is tested in Figure 12 when  $S_1$  of Phase-A is closed at time  $t = 25$  ms. In the simulation result both differential relay and PAD scheme can see the fault, but with different time instants. In this case, PAD scheme signal is the same final tripping signal and it can lead to disconnect the power transformer from total power system with fast response.

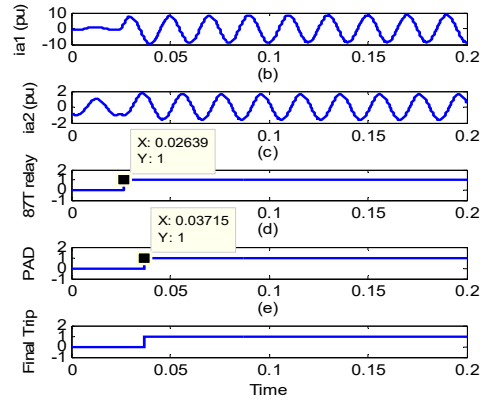


Figure 12. Response of the PAD-based algorithm to turn-to-turn fault

#### 4.5. External fault (ACG fault)

The PAD based algorithm is also tested for external fault (ACG). This fault is located on the low-voltage terminals of the power transformer, and it is initiated at 25 ms, with fault resistance  $0.001 \Omega$ . The status of the proposed relay is shown in Figure 13. As seen, the final trip signal is zero logic because the  $CT_1$  and  $CT_2$  currents flow in the same direction and less than 20 pu.

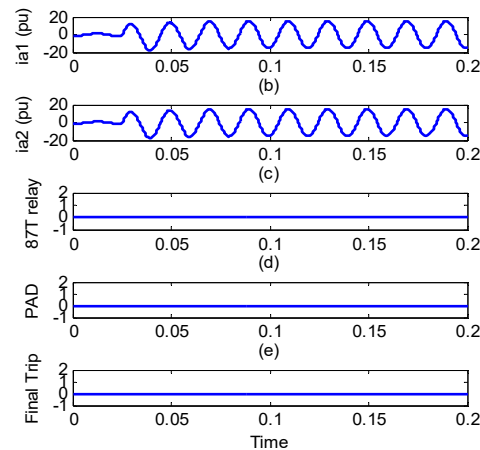


Figure 13. Response of the PAD-based algorithm to AC-G external fault

## 5. CONCLUSION

In this paper the transformer differential protection with PAD based algorithm is modeled by Simulink package. In Simulink model, the power transformer and all current transformers are represented by real equivalent circuit. Also, non-linear inductance is used to represent the magnetization effects. This nonlinearity causes mal-operation in percentage differential relay. The algorithm of transformer differential protection relay was developed by adding PAD based algorithm; this improvement is used to solve the mal-operation of transformer differential protection on magnetizing inrush currents. The Simulink model is simulated at different modes: normal loading, inrush currents and internal and external faults. The simulation results show that the proposed algorithm has good reliability, largely independent of harmonic contents in the

differential current, and transformer parameters. Simulink model shows that the proposed algorithm does not require complex computation and can be easily incorporated into existing digital differential relays.

## APPENDIX

Table 1 Power System Parameters

Parameters	value
Source1:	Es =138kV <sub>L</sub> 0o /50Hz ,R+=7.1Ω, L+=53.99mH R0=7.1596Ω, L0=115.45mH
Source2:	Er =13.8kV <sub>L</sub> 20o /50Hz ,R+=1.4Ω, L+=5.6mH R0=1.498Ω, L0=11.975mH
Power Transformer	25MVA, 138kV/13.8kV,R1=0.908Ω, R2=0.0091Ω L1=78.51mH, L2=0.7851mH, Rc=1.19MΩ Lm=flux/current (pu) / Figure 6(b).
CT1: 100/5 A	25VA, 0.25/5 V , 50Hz, R1=2.5μΩ, R2=1mΩ L1=0.31831μH, L2=0.12732mH, Rc=0.25Ω Lm=flux/current (pu) / Figure 6(c).
CT2: 1200/5A	25VA, 0.020833/5 V , 50Hz, R1= 17.361nΩ, R2=1mΩ, L1=2.2105nH, L2=0.12732mH Rc=1.7361mΩ, Lm=flux/current (pu) / Figure 6 (c).
Line parameters	R0 = 0.1437Ω, R1 = 0.3101 Ω L0 = 11.45 mH, L1 = 2.41 mH, C0 = 5.635 nF, C1 = 26.8 nF , length= 1km.

## REFERENCES

- [1] A. Hosny, and V.K. Sood, "Transformer differential protection with phase angle difference based inrush restraint" *Electric Power Systems Research*, vol. 115, pp. 57-64, 2014.
- [2] S.H. Horowitz, A.G. Phadke, *Power System Relaying*, 3rd ed., John Wiley & Sons Ltd, pp.195-201, 2008.
- [3] N. Yadaiah, and N. Ravi, "Internal fault detection techniques for power transformers", *Applied Soft Computing*, vol. 11 pp. 5259-5269, 2011.
- [4] A.M. Mahmoud, M.F. El-Naggar, and E.H. Shehab\_Eldina, "A New Technique for Power Transformer Protection Based on Transient Components", *International Conference on Advances in Energy Engineering, IC/AEE*, pp. 318-324, 2011.
- [5] Wiszniewski, A. and Kasztenny, B. "A multi-criteria differential transformer relay based on fuzzy logic". *IEEE Transactions on Power Delivery*, 10(4), pp.1786-1792, 1995.
- [6] Tripathy, M. "Power Transformer Differential Protection Based on Neural Network Principal Component Analysis, Harmonic Restraint and Park's Plots". *Advances in Artificial Intelligence*, pp.1-9, 2012.
- [7] Krishnamurthy, S., Elenga Baningobera, B. IEC61850 "standard-based harmonic blocking scheme for power transformers". *Prot Control Mod Power Syst*, 4, 10, 2019.
- [8] Gouda, O.E., El Dein, A.Z. & Moukhtar, I. "Performance of transformer differential relay at different neutral grounding resistance based on wavelet transform". *Electr Eng* 99, 275-284, 2017.
- [9] Krstivojevic, J., & Djuric, M. "A new algorithm for avoiding maloperation of transformer restricted earth fault protection caused by the transformer magnetizing inrush current and current transformer saturation". *Turkish Journal of Electrical Engineering & Computer Sciences*, 24, 5025-5042, 2016.
- [10] Kaur, A., Brar, Y., & G., L. "Fault detection in power transformers using random neural networks". *International Journal Of Electrical And Computer Engineering (IJECE)*, 9(1), 78. doi: 10.11591/ijece.v9i1. pp. 78-84, 2019.
- [11] Outzguinrimt, H., Chraygane, M., Lahame, M., Oumghar, R., Batit, R., & Ferfra, M. "Modeling of three-limb three-phase transformer relates to shunt core using in industrial microwave generators with n=2 magnetron per phase". *International Journal of Electrical and Computer Engineering (IJECE)*, 9(6), 4556. doi: 10.11591/ijece.v9i6. pp4556-4565, 2019.
- [12] J.K. Bladow, A. "Montoya Experiences with parallel EHV phase shifting transformer IEEE Trans". *Power Deliv.*, 6 (3), pp. 1096-1100, 1991.
- [13] Alsharif, M., Yahya, K. and Geem, Z., "Strategic Market Growth and Policy Recommendations for Sustainable Solar Energy Deployment in South Korea". *Journal of Electrical Engineering & Technology*, 2019.
- [14] Jebur, I. and Hameed, K. "Evaluation and improvement of the main insulation structure of 33kV distribution transformer based on FEM". *Indonesian Journal of Electrical Engineering and Computer Science (IJECS)*, 15(1), p. 36, 2019.
- [15] Kareem, O., Adekitan, A. and Awelewa, A. "Power distribution system fault monitoring device for supply networks in Nigeria. *International Journal of Electrical and Computer Engineering (IJECE)*, 9(4), p. 2803, 2019.
- [16] Badri, R. and Hocine, L., "Diagnosis winding short-circuit faults of power transformer". *Global Journal of Computer Sciences: Theory and Research*, 8(2), pp.70-78, 2018.

- [17] S. Hodder, B. Kasztenny, N. Fischer, and Y. Xia “Low Second-Harmonic Content in Transformer Inrush Currents-Analysis and Practical Solutions for Protection Security”, presented at the *IEEE 2014 Texas A&M Conference for Protective Relay Engineers*, 2014.
- [18] ABB power T&D Company Inc. “Type 87T-Circuit Shield-Transformer Differential Relay”, *I.B.* 7.6.1. pp. 7-4, Issue B.
- [19] Werstiuk, C. “The relay testing handbook. Arvada”, CO: Valence Electrical Training Services, 2012.
- [20] A. Guzman, N. Fischer and C. Labuschagne, "Improvements in transformer protection and control," 2009 *62nd Annual Conference for Protective Relay Engineers*, Austin, TX, pp. 563-579, 2009.
- [21] Hermanto, M.Y. Murty, and M.A. Rahman, “A stand-alone digital protective relay for power transformers”, *IEEE Trans. Power Deliv.* vol. 6, pp. 85-95, 1991.
- [22] Iqteit NA, Arsoy AB, Çakir B. “A simple method to estimate power losses in distribution networks”. *Proc. of 10th International Conference on Electrical and Electronics Engineering (ELECO)*, Bursa, Turkey 2017: 135-140.
- [23] N. Yadaiah, N. Ravi, “Internal fault detection techniques for power transformers”, *Applied Soft Computing*, vol. 11, pp. 5259-5269, 2011.
- [24] A. Ngaopitakkul, and A. Kunakorn, “Internal Fault Classification in Transformer Windings using Combination of Discrete Wavelet Transforms and Back-propagation Neural Networks”, *International Journal of Control, Automation, and Systems*, vol. 4, pp. 365-371, June 2006.
- [25] Jabloski, M. and Napieralska-Juszczak, E. “Internal faults in power transformers”. *IET Electric Power Applications*, 1(1), p. 105, 2007.
- [26] Hosny, A. and Sood, V. “Transformer differential protection with phase angle difference based inrush restraint”. *Electric Power Systems Research*, 115, pp.57-64, 2014.